Available online at www.sciencedirect.com

ScienceDirect

Energy Procedia 105 (2017) 4295 – 4304

Energy Procedia

The 8th International Conference on Applied Energy – ICAE2016

A new approach for the dimensioning of an air conditioning system with cold thermal energy storage

Luigi Mongibello[a,*], Nicola Bianco[b], Martina Caliano[b], Giorgio Graditi[a]

[a]*ENEA Italian National Agency for New Technologies, Energy and Sustainable Economic Development - Portici RC, 80055 Portici (NA), Italy*

[b]*Dipartimento di Ingegneria Industriale (DII) – Università degli Studi Federico II, 80125 Napoli, Italy*

Abstract

In this work, a new approach for the design of air conditioning systems with cold thermal energy storage is described and tested, considering the case study represented by a vapor-compression chiller, coupled with a chilled water storage system, producing cooling for a small multi-apartment building situated in Italy. In the present approach, at the aim of limiting shut-downs and start-ups of the chiller, which involve inefficiencies during transients, and can lead to a drastic reduction of the equipment lifetime, the nominal power of the chiller, and the amount of cooling to be stored are first estimated in a pre-design phase. Successively, the outputs of the pre-design are used to fix the size of the cold storage tank, and to set up the numerical simulation of the cold thermal energy storage system. Finally, the results of the numerical simulation of the cold storage system are used to evaluate the effective size of the chiller. Both the pre-design and the numerical simulations of the cold storage systems have been done by means of home-made numerical tool realized with Simulink.

In the paper, the specifications relative to the operational strategy are explored, and the analytical models used for the numerical simulation of the cold storage system relative to the Italian case study are reported in detail. Finally, the results of the pre-design, and of the cold storage system simulations relative to the case study are presented and discussed. The results relative to the Italian case study demonstrates the effectiveness of the present approach in limiting the number of shut-downs and start-ups of the chiller.

The present approach can represent a useful tool for the economic optimization of the design of air conditioning systems.

Peer-review under responsibility of the scientific committee of the 8th International Conference on Applied Energy.

Keywords: cold storage ; chilled water ; partial storage strategy ; numerical simulation

* Corresponding author. Tel.: +39-081-7723584; fax: +39-081-7723345.
E-mail address: luigi.mongibello@enea.it.

Peer-review under responsibility of the scientific committee of the 8th International Conference on Applied Energy.
doi:10.1016/j.egypro.2017.03.900

1. Introduction

Cold thermal energy storage (CTES) in HVAC&R systems can allow to shift the electric demand/electric rate fully or partially from on-peak hours to off-peak ones. This generally implies a reduction of the operating costs and of the equipment ones, since thermal energy storage allows to reduce the equipment size, and to have longer operating hours of compressors and pumps, and chillers and cooling towers at full load at lower outdoor temperatures during nighttime. Nevertheless, in general the use of thermal energy storage systems also presents some drawbacks, which essentially are the high initial costs, complicated operation, maintenance and control, and high encumbrance [1,2]. For a generic application, the design of such a system is strongly interconnected with the operation strategy, that can follow a full storage or a partial storage approach, depending essentially on the user demand, the electricity tariffs, and the equipment efficiencies and costs.

The effectiveness of cold storage in obtaining a profitable peak load shifting for refrigeration systems has been demonstrated by a number of works. Many control strategies and several storage materials have been tested to the purpose, with chilled water and ice being the most used cold storage materials. Lin et al. [3] conducted a thermo-economic analysis of an air conditioning system with chilled water storage, in which part of the chilled water back from the user is mixed to the chilled water supplied to the user, and analyzed the thermodynamic performance influence on cost saving. Yan et al. [4] optimized the design of an air conditioning system based on the use of a seasonal heat pipe-based ice storage system. Following their approach, during winter the seasonal ice storage system collects cold energy from ambient low-temperature air. In summer, ice cold energy is extracted for air conditioning, and the melted ice is used as storage medium for chilled water storage. Soler et al. [5] analyzed the performance of a cooling network composed of eight chillers with different capacities and coefficients of performance, and a storage system, at the aim of maximizing chillers operating efficiency, and minimizing the number of shut-downs and start-ups. Meyer and Emery [6] optimized from the economical point of view the operation of an air conditioning system composed of two chillers, one designated for ice storage charging, the other for direct cooling, an air-handling unit, a cooling tower, and water pumps. Habeebullah [7] investigated the economic feasibility of retrofitting an ice thermal energy storage system for an air conditioning system, considering both full storage and partial storage approach.

In the last years, great attention has been also addressed to phase change materials (PCMs) different from ice, which have the potential to considerably lower the size of the storage, and consequently its encumbrance that represents one of the main limits of such systems [8-10].

In this work, a new approach for the dimensioning of air conditioning systems with cold thermal energy storage is described and tested, considering the case study represented by a vapor-compression chiller coupled with a chilled water cold storage system producing cooling for a small multi-apartment building situated in Italy.

In the first part of the paper, the specifications relative to the operational strategy adopted, and to the analytical models used for the numerical simulation of the cold storage system are discussed. Successively, the user thermal and electricity demand for air-conditioning in the summer season are reported. Finally, the results of the pre-design, and of the cold storage system simulations relative to the case study are presented and discussed.

2. Operation strategy and simulation model

2.1. Operation strategy and pre-design

Considering, for example, an air conditioning system based on an electric chiller and without cold storage, for a generic user and for a fixed set-point of the internal ambient temperature, generally the chiller operation cannot be continuous during the hours characterized by a refrigeration load that is lower than the minimum chiller thermal power. Indeed, in those hours, the controller of the air conditioning system would switch off the system each time the user internal ambient temperature reaches the predetermined set-point.

In the present approach for the dimensioning of an air conditioning system with cold thermal energy storage, in order to limit the number of shut-downs and start-ups of the chiller, the nominal power of the chiller, and the amount of cooling to be stored are calculated, in a pre-design phase, applying the following operation constraints: during its operation, the chiller has to work at constant power; the chiller cannot feed the cold storage system only, that, in other words, means that cooling can be accumulated only when the chiller has to feed the user; the ratio between the cooling power transferred to the user and the chiller power has to be higher than or equal to a predetermined minimum value, otherwise the chiller is shut down. Successively, the outputs of the pre-design are used to fix the size of the cold storage tank, and to set up the numerical simulation of the cold thermal energy storage system. Finally, the numerical results are used to evaluate the effective size of the chiller.

2.2. Chilled water storage tank model

One-dimensional analytical models have been used in order to simulate the cold water storage tank and the coiled tube heat exchanger [11]. Fig. 1 shows a sketch of the close vertical cylindrical tank with a single immersed serpentine considered in the present study.

The internal water volume is divided into isothermal nodes representing water layers of equal volume. The energy balance for each node is written as:

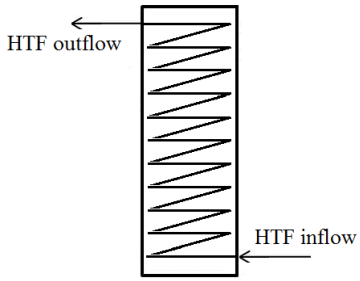

Fig. 1. Sketch of the cold water storage tank

$$\rho_w V_w c_{p_w} \frac{dT_w}{dt} = \frac{(T_{HTF} - T_w)}{R_{coil}} + Q_{cond} - \frac{(T_w - T_{amb})}{R_{tank}} \quad (1)$$

where Q_{cond} represents the conductive heat exchange with adjacent layers. The thermal resistance relative to each layer of the storage wall has been evaluated as:

$$R_{tank} = R_{conv\_int} + R_{cond} + R_{conv\_ext} \quad (2)$$

where

$$R_{conv\_int} = \frac{1}{\bar{h}_{int\_tank} A_{int\_tank}} \tag{3}$$

The mean convective heat transfer coefficient relative to the inner tank wall in equation (3) is evaluated using the Nusselt number correlation for free convection relative to vertical flat plate [12].

The conductive thermal resistance relative to the tank wall has been evaluated as:

$$R_{cond} = \frac{ln\left(\frac{r_{out\_tank}}{r_{in\_tank}}\right)}{2\pi k_{ins} \Delta_{layer}} \tag{4}$$

It has been assumed that the tank thickness is equal to the insulation thickness (0.1m, expanded polyurethane), namely that the conductive thermal resistance relative to the tank steel wall is negligible.

The convective thermal resistance relative to the external tank wall has been evaluated as:

$$R_{conv\_ext} = \frac{1}{\bar{h}_{ext\_tank} A_{ext\_tank}} \tag{5}$$

For each time-step and for each node, the energy balance equations system composed of equation (1) written for all nodes is solved using the implicit Euler method. The empirical reversion-elimination algorithm [13,14] has been adopted in order to include the effects of natural convection heat transfer between the water layers at different heights on the thermal stratification inside the tank.

A transient one-dimensional model has been adopted for the evaluation of the temperature field of the heat transfer fluid (HTF) flowing through the immersed coil heat exchanger.

Also the heat exchanger has been divided in isothermal nodes representing tube sections having the same volume. For each node, the energy balance equation is given by:

$$\rho_{HTF} V_{nod} c_{p_{HTF}} \frac{dT_{HTF}}{dt} = \frac{\left(T_{tank} - T_{HTF}\right)}{R_{coil}} + \rho_{HTF} \dot{V}_{HTF} c_{p\,HTF} \left(T_{HTF\_in} - T_{HTF\_out}\right) \tag{6}$$

The thermal resistance between the HTF in the coil heat exchanger and the water in the cold storage tank is given by:

$$R_{coil} = R_{conv\_int} + R_{conv\_ext} + R_{cond} \tag{7}$$

where

$$R_{conv\_int} = \frac{1}{\bar{h}_{int\_coil} A_{int\_coil}} \tag{8}$$

The mean internal convective heat transfer coefficient in equation (8) is evaluated using the Gnielinski's correlation for coiled tube heat exchanger [15] for the Nusselt number calculation.

The external convective thermal resistance has been evaluated as:

$$R_{conv\_ext} = \frac{1}{\bar{h}_{ext\_coil} A_{ext\_coil}} \tag{9}$$

The mean external convective heat transfer coefficient in equation (9) is evaluated using the Morgan's correlation for natural convection for horizontal cylinders [16] for the evaluation of the Nusselt number.

The conductive thermal resistance of the coil has been neglected, because its order of magnitude is much lower than the internal and external convective thermal resistances.

For each time-step and for each node, equation (6) is solved using the implicit Euler method.

The coupling between the cold water tank balance equations system and the one relative to the serpentine has been dealt with an iterative approach.

3. Case study

In the analysed application, the user is represented by a small multi-apartment building, characterized by a total surface area equal to 800 m^2 and an envelope shape factor of 0.5 m^{-1}, and situated in the Italian climatic zone E. The yearly thermal energy demand and the daily thermal and electrical load profiles for the air conditioning in the warm season have been evaluated as in reference [17]. In particular, it has been considered that the air conditioning in the warm season is realized by means of an electrical vapour-compression chiller with a hydronic loop, the yearly thermal energy demand is 21 kWh/m^2/yr, and that the daily thermal and electrical load profiles are the same for all the operation days. Fig. 2 shows the hourly averaged thermal and electrical load profiles for refrigeration relative to the user for the standard day considered.

The electrical load profile has been evaluated considering the EER of the chiller depending on the ambient temperature. Fig. 3 shows the variation of the EER as a function of the hourly averaged ambient temperature. In this figure, the temperature profile and the EER one are normalized using the maximum average temperature equal to 28°C, and the maximum value of EER equal to 3, respectively. Thus, with reference to the Fig. 2, and without considering a cold storage integrated into the refrigeration system, for the present user it is necessary a chiller of 7.9 kW of nominal electric power in order to fulfill the request for air conditioning in the summer season.

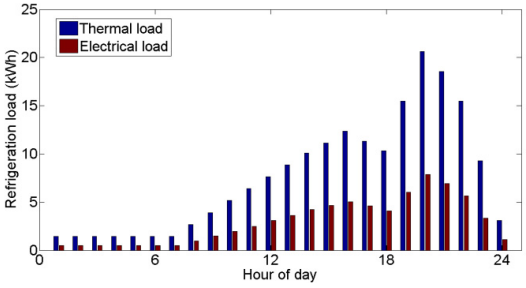

Fig. 2. Refrigeration load of the user

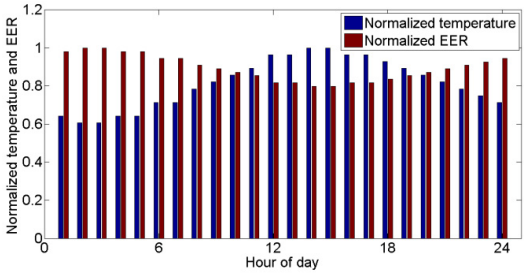

Fig. 3. Non-dimensional temperature and EER profiles

4. Results

4.1. Pre-design and operation strategy implementation

Fig. 4 shows the thermal and electrical powers of the chiller through the day, resulting from the pre-design relative to the considered case study, obtained by fixing the minimum ratio between the cooling power to the user and the chiller power to 0.5, while Fig. 5 shows on the same graph the resulting chiller thermal power and the refrigeration loads. It can be noticed the peak-shaving effect due to the cold storage. Fig. 6 shows, for each hour of the day, the minutes of continuous operation of the chiller. It can be noticed that the present operation strategy involves only 10 shut-downs and start-ups a day, However, it can be also seen that a large part of the chiller production still remains concentrated in the on-peak hours.

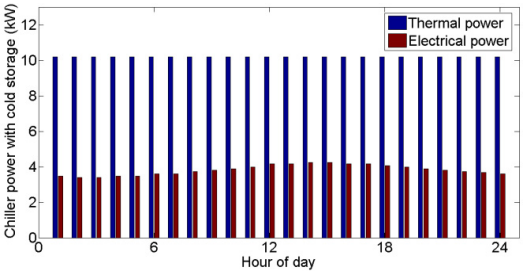

Fig. 4. Chiller power with cold storage

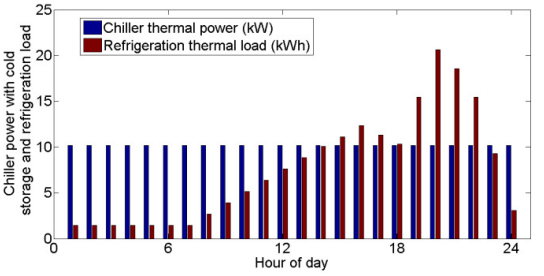

Fig. 5. Chiller thermal power and refrigeration loads

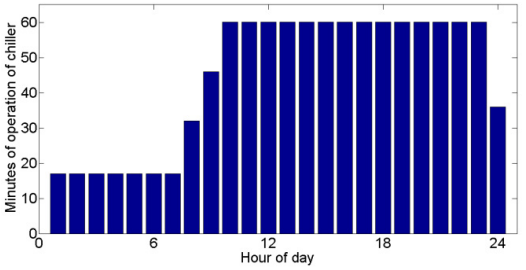

Fig. 6. Minutes of operation of the chiller

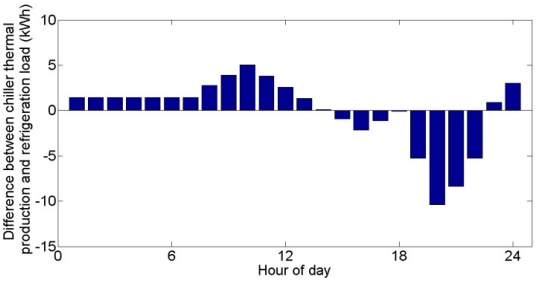

Fig. 7. Difference between the chiller thermal production and the refrigeration loads

Fig. 7 shows, for each hour of the day, the difference between the chiller thermal production and the refrigeration load. Thus, with the adopted approach, the resulting chiller thermal power for the refrigeration system with cold storage is constant and equal to 10.2 kW, with a maximum absorbed electric power of 4.2 kW, that is about the half of the maximum electric power that is needed in the case without the cold storage. The resulting amount of cooling to be stored is 33.6 kWh, that is about the 18% of the user daily total request.

The implementation of the above operation strategy, as well as the numerical simulation of cold storage system, has been performed by means of a home-made tool realized in Simulink. To the purpose, with reference with the simplified layout of the refrigeration system shown in Fig. 8, it has been assumed that the HTF exits the chiller at a constant temperature $T_{c,out}$=7.0°C, and at a constant flowrate of 0.4 kg/s.

Owing to the assumption of constant chiller thermal power, the expected temperature of the HTF at the inflow section of the chiller is equal to $T_{c,in}$=13.1°C. The operation constraint of fixing the minimum ratio between the cooling power to the user and the chiller power to 0.5 is equivalent to fixing the minimum ratio between the mass flow rate through the user and the mass flow rate through the chiller to 0.5.

During chiller operation, the mass flow rate of HTF through the user is controlled by means of valve V1 so that the temperature at the user exit, i.e. at point A, is equal to $T_{c,in}$. In case the valve V1 is partially open, the HTF passing through V1 goes to the cold storage tank charging it. A further control is applied by means of valve V2 in order to maintain the temperature at point B equal to $T_{c,in}$. In this case the valve V3 is fully open while valve V4 is fully close.

Otherwise, in case valve V1 is fully close, which implies that all HTF from the chiller goes to the user and that the HTF exits the user at a temperature that is higher than $T_{c,in}$, the cold storage tank is discharged.

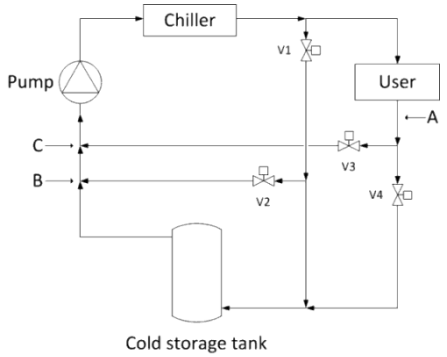

Fig. 8. Layout of the refrigeration system

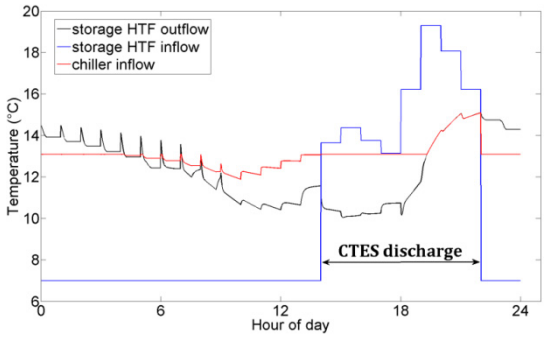

Fig. 9. HTF temperature profiles at the tank heat exchanger inflow and outflow sections, and at the chiller inflow section

In this case, a control is applied by means of valve V3 in order to maintain the HTF temperature at point C equal to $T_{c,in}$, and valve V2 is fully closed.

4.2. Cold storage tank numerical simulation

The size of the water tank is calculated by using the value of the cooling to be stored coming from the pre-design, i.e. 33.6 kWh, and the difference between the HTF inflow and outflow temperatures relative to the chiller, namely 13.1°C and 7°C, respectively. The resulting water volume is equal to about 4.8 m^3. Finally, a commercial cylindrical tank with a capacitance of 4 m^3 has been used for the simulations. The tank height from its bottom surface is equal to 2.55 m (not including insulation), and the entire external surface of the tank is insulated by means of a 0.1 m layer of rigid expanded polyurethane. The tank is provided with a single 1" serpentine with a heat exchange surface of 12 m^2, and the tank capacitance does not include the volume occupied by the serpentine. The inflow section of the serpentine is placed at 5 cm from the tank bottom surface, while the outflow one at 5 cm from the tank top surface. The results of the numerical simulation presented in this section refer to a spatial discretization of the tank realized using 50 nodes, while the serpentine discretization has been made so that its nodes represent the serpentine portions included in the tank layers relative to the tank nodes. A time-step of 60 s has been adopted. Independency of results from the spatial discretization and time-step has been assured.

At each time-step, the HTF mass flow rate flowing through the tank heat exchanger, and the HTF temperature at the inflow section of the heat exchanger are evaluated according to the operation strategy

reported in section 4.1. The main outputs of the numerical simulation are the temperatures at the tank and serpentine nodes.

The following results refer to periodic conditions, obtained starting from an initial temperature of the tank water and of the HTF in the serpentine equal to 13.1°C.

Fig. 9 shows the temporal evolution of the HTF temperature at the serpentine outflow during the day, the one relative to the HTF temperature at the serpentine inflow, and the resulting temporal evolution of the HTF temperature at the chiller inflow, while Fig 10 shows the HTF mass flow rate through the serpentine and through the user.

In Fig. 9, it can be noticed that, from h=5 to the end of the storage charging phase, the HTF temperature at the chiller inflow is lower than the nominal chiller inflow temperature, i.e. 13.1°C. This is because, in that time interval, the HTF temperature at the serpentine outflow is lower than 13.1°C, implying that the chiller has to work at a lower power in that period in order to maintain the HTF temperature at its outflow constant and equal to 7°C.

It can be also noticed that, at the end of the discharging phase, the HTF temperature at the serpentine outflow, and the one at the chiller inflow are higher than 13.1°C. In this case, the chiller has to work consuming a higher electrical power than the one evaluated in the pre-design, up to 6.1 kW, in order to keep the outflow temperature constant and equal to 7°C, implying that the chiller operating at a constant absorbed electric power of 4.2 kW, together with the considered commercial size of the cold storage tank, is not capable to fulfill continuously the user request.

The above consideration are evident if Fig 11, showing the cold energy taken and released from the storage during the day evaluated in the pre-feasibility analysis, and the ones resulting from the numerical simulations, is analyzed. In fact, it can be seen that, at the end of the charging phase, the storage system accumulates less cold than the one resulting from the pre-feasibility analysis. Moreover, it can be seen that at the end of the discharging phase, the cold released by the storage system is much lower than the one evaluated in the pre-feasibility analysis. This results are essentially due to chosen tank size, to the storage degradation due to the cold energy losses through the tank external walls, and to the degradation of the temperature stratification inside the tank. Figure 12 and 13 show the evolution of the water temperature profile in the tank during the charging phase and the discharging one, respectively.

Thus, considering the operation strategy and the size of the cold storage system adopted in this study, in the case with cold storage it is necessary to have a chiller, provided with an inverter, characterized by a maximum absorbed electric power of 6.1 kW, that, however, is well below the one relative to the case without the cold storage, namely 8 kW. Table 1 shows the storage tank and chiller sizes obtained by varying the minimum ratio between the cooling power transferred to the user and the chiller power.

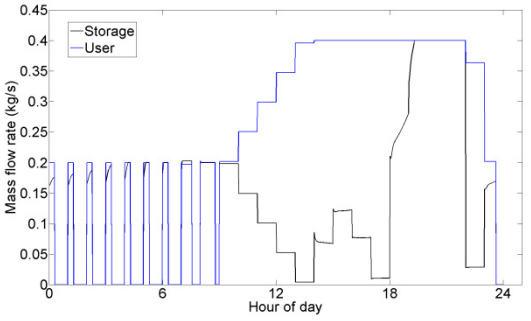

Fig. 10. HTF mass flow rate through the tank heat exchanger and the user

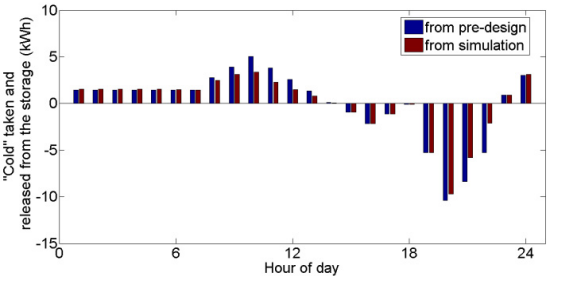

Fig. 11. Cooling energy taken and released from the cold water tank

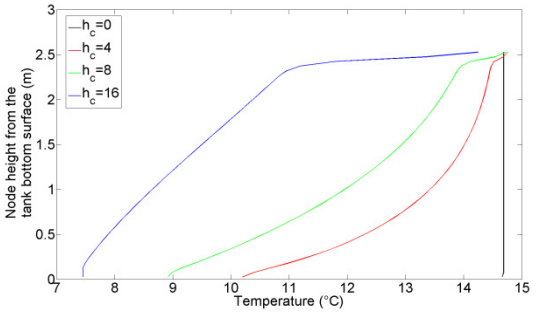

Fig. 12. Temperature profiles in the cold water tank during the charging phase (h_c=0 refers to the beginning of the phase)

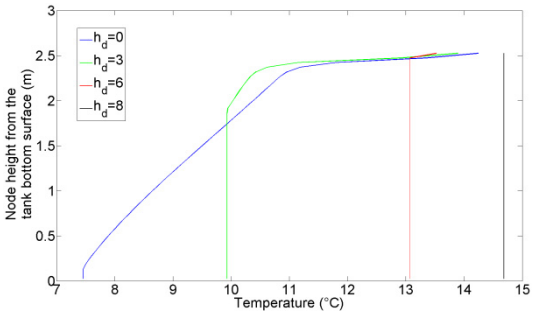

Fig. 13. Temperature profiles in the cold water tank during the discharging phase (h_d=0 refers to the beginning of the phase)

Table 1. Main results by varying the minimum ratio between the cooling power transferred to the user and the chiller power

Minimum ratio between the cooling power transferred to the user and the chiller power	Storage capacity (pre-design) (kWh)	Storage volume (pre-design) (m^3)	Storage volume (simulation) (m^3)	Chiller powers (pre-design) (kW_t , kW_e)	Chiller power (simulation) (kW_t , kW_e)
0	59.9	11.4	8.0	(7.6 , 3.2)	(11.5 , 4.8)
0.25	51.84	8.85	8.0	(8.3 , 3.5)	(11.4 , 4.7)
0.5	33.60	4.80	4.0	(10.2 , 4.2)	(13.5 , 5.6)
0.75	23.35	2.85	2.0	(11.8 , 4.9)	(15.1 , 6.3)
1	0	0	-	(20.6 , 7.9)	-

5. Conclusion

In this work, a new approach for the design of air conditioning systems with cold thermal energy storage is described and tested, considering the case study represented by a vapor-compression chiller, coupled with a chilled water storage system, producing cooling for a small multi-apartment building situated in Italy.

The specifications relative to the operational strategy have been reported, and the characteristics of the analytical models used for the numerical simulation of the cold storage system relative to the Italian case study have been shown as well. The results relative to the Italian case study have demonstrated the effectiveness of the present approach in limiting the number of shut-downs and start-ups of the chiller.

References

[1] Silvetti B, MacCracken M. Thermal storage and deregulation. *ASHRAE Journal*, 1998;**4**:55–59.
[2] Wang SK. *Handbook of air conditioning and refrigeration*. 2nd ed. New York: McGraw-Hill; 2001.
[3] Lin H, Li XH, Cheng PS, Xu BG. Thermoeconomic evaluation of air conditioning system with chilled water storage. *Energy Conversion and Management*, 2014;**85**: 328–32.
[4] Yan C, Shi W, Li X, Zhao Y. Optimal design and application of a compound cold storage system combining seasonal ice storage and chilled water storage. *Applied Energy*, 2016;**171**:1–11.
[5] Soler MS, Sabaté CC, Santiago VB, Jabbari F. Optimizing performance of a bank of chillers with thermal energy storage. *Applied Energy*, 2016;**172**:275–85.
[6] Kintner-Meyer M, Emery A. Optimal control of an HVAC system using cold storage and building thermal capacitance. *Energy and Buildings*, 1995;**23**(1):19–31.
[7] Habeebullah BA. Economic feasibility of thermal energy storage systems. *Energy and Buildings*, 2007;**39:**355–63.
[8] Sun Y, Wang S, Xiao F Gao D. Peak load shifting using different cold thermal energy storage facilities in commercial buildings: A review. *Energy Conversion and Management*, 2013;**71**:101–14.
[9] Navidbakhsh M, Shirazi A, Sanaye S. Four E analysis and multi-objective optimization of an ice storage system incorporating PCM as the partial cold storage for air-conditioning applications. *Applied Thermal Engineering*, 2013;**58**(1-2): 30–41.
[10] Oró E, Depoorter V, Plugradt NSJ. Overview of direct air free cooling and thermal energy storage potential energy savings in data centres. *Applied Thermal Engineering*, 2015;**85**:100–110.

[11] Mongibello L, Bianco N, Caliano M, de Luca A, Graditi G. Transient analysis of a solar domestic hot water system using two different solvers. Energy Procedia, 2015;**81**:89-99.
[12] Bejan A, Kraus AD. *Heat Transfer Handbook*, Hoboken: John Wiley & Sons Inc. 2003.
[13] Mather DW, Hollands KGT, Wright JL. Single- and Multi-Tank energy storage for solar heating systems: Fundamentals. *Solar Energy* 2002;**73**:3-13.
[14] Newton BJ, Schmid M, Mitchell JW, Beckman WA. Storage tank models. *Proceedings of ASME/JSME/JSES International Solar Energy Conference* 1995, Maui, Hawaii.
[15] Gnielinski Y. Heat transfer and pressure drop in helically coiled tubes. *8th International Heat Transfer Conference* 1986;6:2847–54.
[16] Morgan VT. The overall convective heat transfer from smooth circular cylinders. *Adv. Heat Transfer* 1975;11:199-264.
[17] Mongibello L, Bianco N, Caliano M, Graditi G. Influence of heat dumping on the operation of residential micro-CHP system. *Applied Energy*, 2015;**160**:206–20.

Acknowledgement

This work was funded within the Italian Research Program “Ricerca di Sistema Elettrico – PAR 2015, Area: Efficienza energetica e risparmio di energia negli usi finali elettrici ed interazione con altri vettori energetici”.

Biography

Luigi Mongibello, PhD. He graduated in aerospace engineering at the University of Naples “Federico II” (Italy) in 2002, where he completed, in 2005, a doctorate in aerospace engineering with a thesis on actuators for flow control. His research activities are focused on the experimentation, simulation, and optimization of components and systems for solar collectors, CSP and DES plants, and on the thermal design of PV, BIPV and CPV systems.